The EMBO Journal (2009) 28, 3758–3770 | © 2009 European Molecular Biology Organization | All Rights Reserved 0261-4189/09
www.embojournal.org

THE EMBO JOURNAL

Chaperone proteostasis in Parkinson's disease: stabilization of the Hsp70/α-synuclein complex by Hip

Cintia Roodveldt[1,6,*], Carlos W Bertoncini[1,6], August Andersson[1], Annemieke T van der Goot[2], Shang-Te Hsu[1], Rafael Fernández-Montesinos[3], Jannie de Jong[2], Tjakko J van Ham[2], Ellen A Nollen[2], David Pozo[3], John Christodoulou[1,4,5,*] and Christopher M Dobson[1,*]

[1]Department of Chemistry, University of Cambridge, Cambridge, UK, [2]Department of Genetics, University Medical Centre Groningen and University of Groningen, Groningen, The Netherlands, [3]CABIMER-Andalusian Center for Molecular Biology and Regenerative Medicine (CSIC-University of Seville-UPO-Junta de Andalucia), Seville, Spain, [4]Research Department of Structural and Molecular Biology, Institute of Structural and Molecular Biology, University College London (UCL), London, UK and [5]School of Crystallography, Birkbeck College, University of London, London, UK

The ATP-dependent protein chaperone heat-shock protein 70 (Hsp70) displays broad anti-aggregation functions and has a critical function in preventing protein misfolding pathologies. According to *in vitro* and *in vivo* models of Parkinson's disease (PD), loss of Hsp70 activity is associated with neurodegeneration and the formation of amyloid deposits of α-synuclein (αSyn), which constitute the intraneuronal inclusions in PD patients known as Lewy bodies. Here, we show that Hsp70 depletion can be a direct result of the presence of aggregation-prone polypeptides. We show a nucleotide-dependent interaction between Hsp70 and αSyn, which leads to the aggregation of Hsp70, in the presence of ADP along with αSyn. Such a co-aggregation phenomenon can be prevented *in vitro* by the co-chaperone Hip (ST13), and the hypothesis that it might do so also *in vivo* is supported by studies of a *Caenorhabditis elegans* model of αSyn aggregation. Our findings indicate that a decreased expression of Hip could facilitate depletion of Hsp70 by amyloidogenic polypeptides, impairing chaperone proteostasis and stimulating neurodegeneration.

The EMBO Journal (2009) **28,** 3758–3770. doi:10.1038/emboj.2009.298; Published online 29 October 2009
Subject Categories: proteins; molecular biology of disease
Keywords: amyloid; Hip; Hsp70; Parkinson's disease; α-synuclein

*Corresponding authors. C Roodveldt or CM Dobson, Department of Chemistry, University of Cambridge, Lensfield Road, Cambridge CB2 1EW, UK. Tel.: +44 1223 336366, Fax: +44 1223 336362; E-mail: cintia.roodveldt@cabimer.es or Tel.: +44 1223 763070; Fax: +44 1223 336362; E-mail: cmd44@cam.ac.uk or J Christodoulou, Research Department of Structural and Molecular Biology, Institute of Structural and Molecular Biology, University College London, and School of Crystallography, Birkbeck College, Gower Street, London WC1E 6BT, UK. Tel.: +44 207 6792375; Fax: +44 207 6797193; E-mail: j.christodoulou@ucl.ac.uk
[6]These authors contributed equally to this work

Received: 18 August 2009; accepted: 15 September 2009; published online: 29 October 2009

Introduction

Protein conformational diseases include a range of degenerative disorders in which specific peptides or proteins misfold and aberrantly self-assemble, often in the form of amyloid fibrils, which can be deposited in a variety of tissues, the process of which may lead to toxicity and cell death. These disorders, among others, include Alzheimer's (AD), Parkinson's (PD) and Huntington's diseases (HD) (Chiti and Dobson, 2006; Luheshi *et al*, 2008). One of the most studied amyloid-forming proteins involved in neurodegeneration is α-synuclein (αSyn), the aggregation of which is linked to the pathogenesis of PD. Indeed, αSyn is the major component of Lewy bodies, the protein-rich aggregates found post-mortem in the brains of patients suffering from PD or a number of related diseases.

The pathological conversion of misfolded proteins into cytotoxic species is modulated by interactions with several proteins, among them are molecular chaperones (Dobson, 2003; Stefani and Dobson, 2003; Young *et al*, 2004; Balch *et al*, 2008), which are now recognized as key players in the avoidance of misfolding and hence in protein homeostasis (Dobson, 2003; Young *et al*, 2004; Balch *et al*, 2008). A very important class of chaperones is the family of stress-inducible 70 kDa heat-shock proteins (Hsp70s), which have a critical function in a range of cellular processes including the folding of newly synthesized proteins (Frydman *et al*, 1994) and the rescue of misfolded proteins (Gragerov *et al*, 1992; Mogk *et al*, 1999), hence avoiding the potentially harmful effects of the aggregation of the latter species (Hartl, 1996). Hsp70 proteins are composed of an N-terminal ATPase domain and a C-terminal substrate-binding domain (SBD), connected by a short linker region (Mayer and Bukau, 2005). Within the SBD, the substrate-binding pocket recognizes unstructured segments in polypeptides (Bukau and Horwich, 1998; Mayer *et al*, 2001) and the current view is that Hsp70 prevents misfolding by binding to certain patterns of hydrophobic and positively charged amino acids in the polypeptide substrate (Rudiger *et al*, 1997a, b; Maeda *et al*, 2007). The ATPase cycle of Hsp70 involves alternation between an ATP-bound or 'open' state, which has lower affinity for substrates, and an ADP-bound or 'closed' state with higher affinity (Mayer and Bukau, 2005). This alternation appears to be achieved by a structural 'coupling' between the ATPase domain and the SBD, driven by an allosteric mechanism that is not yet fully understood (Saibil, 2008). The ATPase cycle is typically modulated by several co-chaperones, most notably Hsp40, resulting in an increase in ATPase activity (Minami *et al*, 1996; Bukau and Horwich, 1998). Other co-chaperones include Bag-1, which functions as a nucleotide-exchange factor (Takayama and Reed, 2001), Hop, which interacts with Hsp70 to enhance certain functions (Scheufler *et al*, 2000), and Hip (or ST13), which binds to the ATPase domain of the chaperone in its ADP-bound state and appears to increase the half-life of substrate complexes (Hohfeld *et al*, 1995).

There seems to be a strong link between problems in the regulation of chaperone function and the panoply of conformational diseases and amyloidoses (Dobson, 2003; Macario and De Macario, 2007). For example, patients with PD show highly perturbed expression of Hsp70 in the *substantia nigra*, which is the site of neurodegeneration in this condition (Grunblatt *et al*, 2001; Hauser *et al*, 2005). Indeed, Hsp70 has been found in deposits in the brain of AD patients, in polyglutamine aggregates of sufferers of HD, and in Lewy bodies from PD patients (Muchowski and Wacker, 2005). Furthermore, in PD fly models (Auluck *et al*, 2002) and in human neuroglioma cells (Klucken *et al*, 2004; Zhou *et al*, 2004), over-expression of Hsp70 has been found to reduce significantly the toxicity linked to αSyn. Also, it is particularly interesting that the co-chaperone Hip is consistently present at lower levels in the blood of PD patients relative to healthy controls, even at the early stages of the disease (Scherzer *et al*, 2007).

Despite the compelling *in vivo* evidence of the implications of Hsp70 in disease, *in vitro* studies of the molecular mechanisms of the Hsp70-mediated inhibition of amyloid formation are relatively sparse. For example, the nature of the misfolded species recognized by Hsp70 and of the complexes formed during amyloid aggregation of polypeptides, are not yet known. Equally important is the need to understand the ways in which nucleotides control the interactions with amyloidogenic protein substrates and the potentially important functions by co-chaperones in assisting Hsp70 in its amyloid-inhibiting functions. In this work, we consider the impact of different nucleotide conditions and of co-chaperones on the anti-aggregation activity of Hsp70. Using αSyn as the substrate, we have probed substrate–chaperone interactions for Hsp70 as a function of the nucleotide state of the chaperone and the different species of αSyn attained along the aggregation pathways. By using fluorescence and NMR spectroscopy, we have characterized a structurally compact ADP-Hsp70/αSyn complex that may promote the co-aggregation of Hsp70 and may therefore lead to chaperone depletion. We further identify an important function for the co-chaperone Hip in sustaining the Hsp70-mediated anti-amyloid activity, both *in vitro* and *in vivo*, the latter studies by means of a *Caenorhabditis elegans* model of αSyn aggregation, and speculate that this specific co-chaperone could have an important function in the onset and progression of PD.

Results

The dependence of the solubility and anti-amyloid activity of Hsp70 on binding of nucleotides

To study the effects of ATP on the anti-aggregation activity of Hsp70, a series of *in vitro* aggregation experiments were set up in which αSyn amyloid formation was monitored by thioflavin T (ThT) fluorescence (Figure 1A). The presence of nucleotide-free chaperone at even a 1:10 molar ratio (Hsp70:αSyn) dramatically inhibited amyloid formation, an observation in agreement with our earlier work (Dedmon *et al*, 2005). Interestingly, however, addition of 2 mM ATP (using an ATP-regeneration system, see Materials and methods) to the solution containing Hsp70 was found to inhibit αSyn aggregation initially, but at longer times an increase in ThT fluorescence is evident, indicating the onset of aggregation. Analysis of the kinetics of αSyn aggregation in the presence of various molar ratios of Hsp70 (Figure 1B; Supplementary Figure 1) shows that, in the presence of ATP, both the lag phase and half-time for aggregation increase as the concentration of Hsp70 is increased. The rate of aggregation was also found to be affected by the presence of Hsp70, being reduced by ca. 60–70%, although in a concentration-independent manner (Supplementary Figure 1). Transmission electron microscopy (TEM) was used to assess the morphology of the species formed during the aggregation reaction (Figure 1D), and revealed that the presence of nucleotide-free Hsp70 strongly abrogates fibril formation and produces exclusively small amorphous aggregates that do not enhance the fluorescence of ThT (Dedmon *et al*, 2005). Conversely, addition of Hsp70 together with ATP was found to result in the formation of fibrillar species, which are indistinguishable from amyloid fibril controls.

Although an Hsp70–nucleotide mixture clearly reduces aggregation, we sought to investigate the origins of the apparent loss with time of chaperone activity of nucleotide-loaded Hsp70. We initially compared the quantity of protein in solution at the beginning and end points of a typical aggregation reaction. Quantitative SDS–PAGE analysis (Figure 1C; Supplementary Figure 2B) of soluble and insoluble fractions generated by low-speed centrifugation showed that a very substantial proportion (~80%) of Hsp70 is present in the insoluble fraction but only when ATP and αSyn are both present. This surprising result suggests that the observed surge of ThT fluorescence in the presence of Hsp70 and ATP after ca. 30 h is likely to be a consequence of αSyn-mediated depletion of Hsp70 in a nucleotide-dependent manner.

To define the contribution of the different nucleotide-bound states along the ATPase cycle to this phenomenon, we conducted aggregation experiments in the absence or presence of ATP, ADP or ATPγS, a non-hydrolyzable analogue of ATP. ATP binds to Hsp70 and its hydrolysis stimulates the cycling between conformations with low affinity (ATP-bound) and high affinity (ADP-bound) for substrates. Addition of ADP is therefore expected to stabilize the high affinity state, and ATPγS to maintain Hsp70 in its low affinity conformation (Mayer and Bukau, 2005). The rise in ThT fluorescence indicates, however, that addition of all three types of nucleotide-loaded Hsp70, but especially ATP and ADP, ultimately results in the formation of αSyn amyloid fibrils (Figure 1E). In addition to this conclusion, analysis by SDS–PAGE of the soluble and insoluble fractions corresponding to the end of the aggregation reaction (Figure 1F; Supplementary Figure 2C) shows that, while Hsp70 remains in solution in the absence of nucleotides, the addition of nucleotides, and ADP in particular, promotes the partitioning of Hsp70 into the aggregated fraction.

We next probed the specificity of the Hsp70/αSyn interaction by assaying the same samples in the presence of the peptide NR (NH_2-NRLLLTG-COOH), that is expected to compete with αSyn for the substrate-binding pocket of Hsp70 (Gragerov *et al*, 1994; Rudiger *et al*, 1997a). The reduction in the level of ThT fluorescence signal at the endpoint of the assay, and an increase in the solubility of the chaperone during the aggregation process, showed clearly that the NR

peptide strongly perturbed the Hsp70/αSyn interactions in the presence of nucleotide (Figure 1E and F; Supplementary Figure 2C). This competitive effect was much more pronounced for Hsp70-ADP than for the other nucleotide-loaded states, a result indicative of interactions between αSyn and the substrate-binding pocket of the chaperone. Under nucleotide-free conditions, on the other hand, the anti-amyloidogenic activity of Hsp70 does not appear to rely on binding to the canonical substrate-binding pocket as under these circumstances the addition of the NR peptide does not influence significantly the efficacy of nucleotide-free Hsp70 in inhibiting fibril formation (Figure 1E and F).

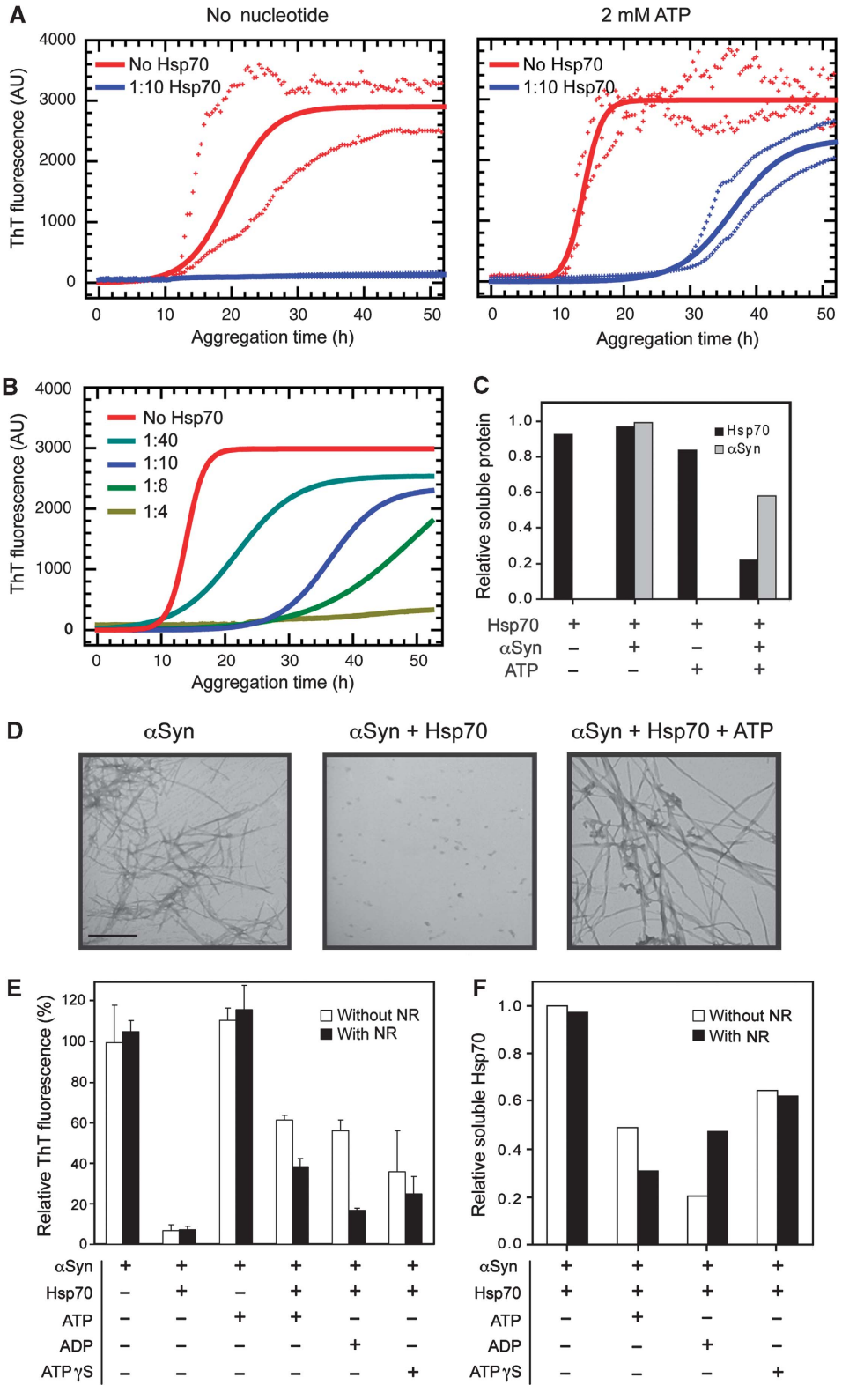

The effect of Hsp70 on the morphology and cytotoxicity of αSyn aggregates

The currently accepted view is that the process of aggregation of αSyn involves the population of oligomeric intermediates that cause cellular damage (Lashuel *et al*, 2002; Danzer *et al*, 2007), which is likely to be a generic feature of such amyloid-related species (Demuro *et al*, 2005; Chiti and Dobson, 2006; Lashuel and Lansbury, 2006; Danzer *et al*, 2007). The nucleotide-dependent anti-aggregation properties of Hsp70 are likely to be reflected in the assembly of different intermediates along the route towards fibril formation. To characterize the properties of species formed during the aggregation of αSyn, we have studied the morphology and monitored the cytotoxicity of the protein adducts formed at early and late stages of the aggregation process under different conditions. Of particular interest is the observation that early αSyn aggregates formed in the presence of Hsp70 and ATP are protofibrillar in nature, whereas only spherical oligomeric species can be observed when the nucleotide-free chaperone is present (Figure 2A and B).

We also assayed the toxicity of the soluble oligomeric prefibrillar adducts formed under a variety of conditions by adding these species, separated by centrifugation from larger aggregates, to human neuroblastoma SH-SY5Y cells in culture

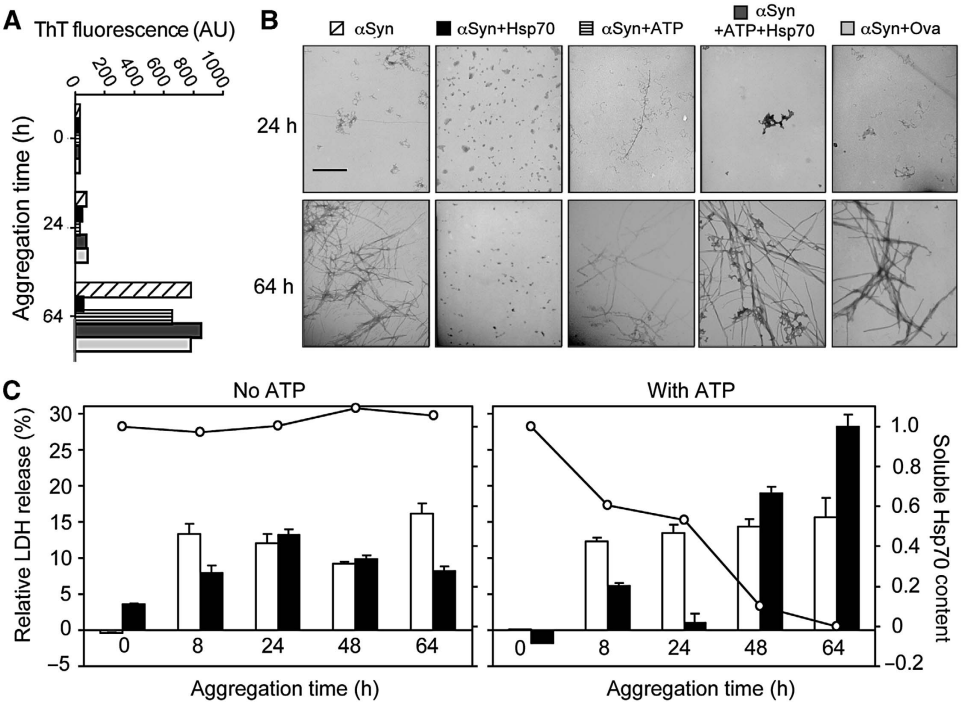

Figure 2 Effect of Hsp70 on the morphology and cytotoxicity of αSyn aggregating species throughout the reaction. (**A**) Fibril formation by αSyn was monitored by ThT fluorescence. Samples correspond to untreated or Hsp70-treated αSyn at a 1:10 ratio, in the absence or presence of ATP. Samples labels in (B). A negative control with added ovalbumin was used. AU, arbitrary units. (**B**) TEM analysis of samples corresponding to 24 and 64 h of the aggregation reaction. A negative control with ovalbumin was also included. Scale bar, 500 nm. (**C**) The toxicity levels of the soluble species from samples corresponding to the different conditions and time points of the reaction were determined by LDH release measurement (left axes) using human SH-SY5Y cells. Samples correspond to untreated αSyn (white bars) or αSyn treated with 1:10 Hsp70:αSyn (black bars), either in the absence (left panel) or presence (right panel) of ATP. The bars represent the intrinsic toxicity, that is the net toxicity (with background toxicity levels subtracted) normalized to the αSyn concentration. In all cases, values represent the average results of duplicate experiments. Connected circles represent the Hsp70 soluble levels at each time point (right axis).

Figure 1 Effect of nucleotides and a competing peptide on the modulation of αSyn aggregation by Hsp70. (**A**) Aggregation experiments of αSyn in the absence or presence of a 1:10 molar ratio of Hsp70 without (left) or with the addition (right) of 2 mM ATP (and an ATP-regeneration system). Fibril formation was monitored by ThT fluorescence. Solid lines correspond to fitted data according to a nucleation-polymerization model and crosses represent the maximum and minimum values measured at each time point. (**B**) Concentration dependence of the Hsp70-ATP anti-amyloidogenic effect. Samples correspond to αSyn alone or with a 1:40, 1:10, 1:8 or 1:4 molar ratio of Hsp70:αSyn, in the presence of 2 mM ATP (and an ATP-regenerating system). Solid lines correspond to fitted data according to a nucleation-polymerization model. (**C**) Densitometric analysis of Hsp70 and αSyn protein bands resolved in an SDS–PAGE corresponding to samples of the soluble fraction at the end of an aggregation reaction, relative to the initial concentration. Where indicated, samples contained a 1:10 molar ratio Hsp70:αSyn (see gel picture in Supplementary Figure 2B). (**D**) Representative TEM images of αSyn aggregates corresponding to the final time point of an aggregation experiment. Samples correspond to untreated αSyn (left), or αSyn treated with a 1:10 Hsp70 ratio either in the absence of added nucleotide (centre) or in the presence of ATP (right). Scale bar: 500 nm. (**E**) Bar diagram representing the relative ThT levels reached at the end of the aggregation reaction. Hsp70 at a 1:10 ratio, and ATP, ADP or ATPγS were included in the reaction mixture where indicated. The NR peptide was included where indicated at a 1:15 molar ratio (Hsp70:NR). Error bars denote one s.d. from the mean, calculated from three independent experiments. (**F**) Densitometric analysis of Hsp70 and αSyn protein bands from an SDS–PAGE gel analysis of samples corresponding to the soluble fraction at the end of the aggregation reaction shown in (E), relative to the initial protein concentration (see gel pictures in Supplementary Figure 2C).

and measuring the release of the enzyme lactate dehydrogenase (LDH) (Figure 2C), which is commonly used as an indicator of cell death. Treatment with Hsp70 alone was observed to reduce cell death only for samples containing soluble intermediates formed very early (8 h) and very late (64 h) in the aggregation process (ca. 40% and ca. 50% decrease in LDH release, respectively), probably caused by a change in the nature of the soluble aggregates present during the course of aggregation. The addition of ATP to the Hsp70-treated sample, however, caused a strong and sustained reduction of toxicity during the lag phase of aggregation ($\leqslant$24 h) (virtually up to 100% suppression), but much later in the aggregation reaction ($\geqslant$48 h) toxicity was again observed to develop. By examining quantitatively the content of soluble Hsp70 at each time point, we can conclude that the capacity of Hsp70 to suppress the toxicity of the oligomeric aggregates of αSyn under the different conditions examined in this study is strongly correlated with its ability to remain in solution and depends on whether nucleotides are present.

Structural features of the interaction between Hsp70 and αSyn

We have shown that nucleotides have profound effects on the anti-amyloidogenic activity of Hsp70 and, in addition, can promote its co-aggregation with αSyn. Next, we looked in detail at the interactions between these two proteins as a function of the nucleotide state of Hsp70. The existence of interactions between Hsp70 and αSyn has been suggested earlier from experiments with cell extracts (Zhou *et al*, 2004) and with live cells (Klucken *et al*, 2006), as well as from studies *in vitro* using purified proteins (Dedmon *et al*, 2005; Huang *et al*, 2006). No interaction of Hsp70 with monomeric αSyn has been reported earlier; however, we here show that such interactions exist by means of band-shift assays and fluorescence spectroscopy (Supplementary data and Supplementary Figure 3A and B). Indeed, we also found evidence of a variety of different complexes being formed along the aggregation pathway of αSyn (Supplementary data and Supplementary Figure 3C and D). The binding affinity of monomeric αSyn for Hsp70 was estimated to lie within the low micromolar range (Supplementary Figure 3B) and to be somewhat higher in the presence of ADP than in the absence of nucleotides ($\sim$1.5-fold), in line with reports on other proteins and model peptides (Palleros *et al*, 1993; Gao *et al*, 1995; Greene *et al*, 1995).

To probe the nature of the various complexes formed between different forms of αSyn and Hsp70, we devised a FRET-based spectroscopic strategy. The two naturally occurring tryptophan residues in Hsp70, Trp90 in the ATPase domain and Trp593 in the SBD, were used as donors, and IAEDANS (5-((2-[(iodoacetyl)amino]ethyl)amino)naphthalene-1-sulfonic acid), a widely used dye with a Förster radius (R_0) of 22 Å (Matsumoto and Hammes, 1975; Jeganathan *et al*, 2006), as an acceptor. In each case, IAEDANS was attached to αSyn through one of four single-cysteine replacements created in the protein (Gln24Cys, Gln62Cys, Asn103Cys and Asn122Cys) (Figure 3A) and FRET experiments were carried out with purified fractions of both monomeric and oligomeric forms of αSyn (Supplementary Figure 3F). For monomeric αSyn-24-AEDANS, large changes (4-fold increase) in FRET efficiency were observed upon addition of nucleotides (Figure 3B), whereas the highest FRET signal was observed when the high or low affinity states in Hsp70 were stabilized with ADP or ATPγS, respectively (Figure 3B; Supplementary Figure 3F). For oligomeric αSyn-24-AEDANS, by contrast, the FRET efficiency was found to be largely nucleotide independent. For αSyn-103-AEDANS, we observed that the FRET efficiency was greatest for the nucleotide-free state of Hsp70, with no significant difference between the monomeric and oligomeric forms of αSyn (Figure 3B).

A Trp90Phe mutant bearing a unique Trp residue located in the SBD (see Supplementary data) was also generated to enable FRET measurements with isolated donor/acceptor pairs. Given that the ADP-state of Hsp70 seems to be a key determinant of the substrate-mediated co-aggregation of the chaperone (Figure 1E and F; Supplementary Figure 2C), we explored its interaction with αSyn in further detail. A large increase in FRET efficiency towards αSyn-AEDANS was observed for the ADP-loaded Trp90Phe mutant compared with that seen with the wild-type chaperone (Figure 3C), indicating that these FRET measurements essentially report on the binding of αSyn to the SBD of Hsp70. Indeed, the NR peptide was found to compete with αSyn-24-AEDANS for binding to Trp90Phe-Hsp70, as the FRET efficiency decreased up to $\sim$25% at a 10-fold molar excess (Figure 3D). Notably, unlabelled αSyn reduced the transfer efficiency by almost 50% under the same conditions, suggesting that monomeric αSyn interacts with Hsp70 with a higher apparent affinity than does the NR peptide. Importantly, independent confirmation of the complex formation in the presence of nucleotide was obtained by heteronuclear NMR spectroscopy (Supplementary data and Supplementary Figure 5). Indeed, by using ^{13}C-detected ^{13}CO-^{15}N (CON) correlation experiments on ^{13}C-^{15}N-labelled αSyn (Hsu, 2009), we found that the addition of Hsp70 and ADP perturbed resonances specifically at the N-terminus and NAC region of αSyn (Supplementary Figure 5A and B).

Mapping the recognition site for Hsp70 on αSyn

We have used an algorithm (Rudiger *et al*, 1997b) to predict the regions of αSyn where binding to Hsp70 is likely to be strongest. Two segments show relatively high scores: residues 32–43 and residues 71–82. The predicted free energies of binding ($\Delta\Delta G$) are -9.7 and -4.3 kJ/mol, respectively (Supplementary Figure 6A).

FRET studies with labelled variants of an αSyn derivative lacking the second putative binding segment, termed ΔNAC (residues 71–82) (Rivers *et al*, 2008), show that, as predicted, this region is involved in the binding process. We found that the interaction of Hsp70 with the ΔNAC αSyn-24-AEDANS mutant is not very different from that of Wt αSyn (Figure 3E). However, the ΔNAC αSyn-103-AEDANS species in the presence of ADP (Figure 3F) shows a dramatic reduction in the FRET efficiency (ca. 70% lower) when compared with full-length αSyn, indicating the importance of the NAC region. Moreover, nucleotide-free Hsp70 shows a slightly higher (ca. 30% greater) FRET with ΔNAC αSyn-103-AEDANS than with the full-length protein. Taken together, these results suggest that both the predicted binding sites are important for the interaction with Hsp70 in the presence of nucleotide. Furthermore, the increase in the relative signals observed under certain nucleotide conditions when removing the NAC region, suggests a competition between the binding sites, and

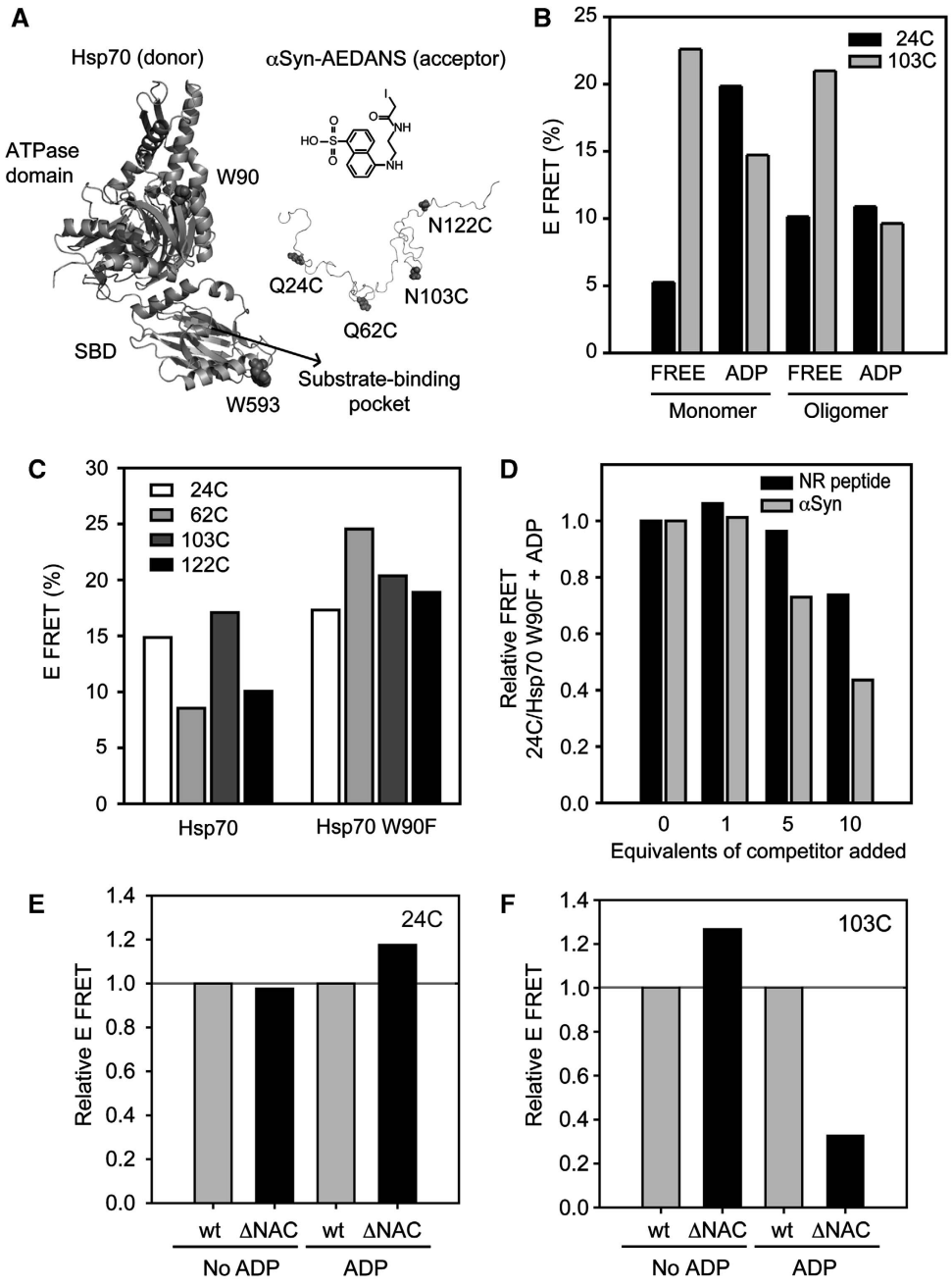

Figure 3 FRET study of Hsp70/αSyn complexes. (**A**) Left, structural model for Hsp70, depicting the ATPase domain, the substrate-binding domain and part of the C-terminal helical lid. The two tryptophan residues are highlighted (solid). The structure of human Hsp70 was modelled by using the Swissmodel web server of Expassy (http://swissmodel.expasy.org/) based on two model templates. Model 1 info: residue range: 1–554 (ATPase and SBD) based on template 1yuw, chain A (2.60 Å) (Hsc70 from *Bos Taurus*); sequence identity [%]: 89; E value: $0.00e^{-1}$. Model 2 info: residue range: 555–634 (C-terminal tail) based on template 1ud0, chain C (3.45 Å) (Hsc70 from *Rattus norvegicus*); sequence identity [%]: 71; E value: $1.20e^{-25}$. Models were created for picturing purposes only. Right, four cysteine replacements in αSyn (solid) allowed targeted attachment to cysteine mutants of the IAEDANS fluorophore, an acceptor of tryptophan fluorescence through FRET ($R_0 = 22$ Å). (**B**) Donor FRET with N-terminally (24C) and C-terminally (103C) tagged αSyn suggests that the modes of binding to Hsp70 differ between the nucleotide-free and ADP-loaded states of the chaperone, and between monomeric and oligomeric forms of αSyn. (**C**) The W90F mutation in Hsp70 allows specific detection of donor FRET with the W593 residue in the SBD of the chaperone. (**D**) The formation of the αSyn-24C-AEDANS/W90F Hsp70 complex is perturbed by addition of the NR peptide, showing the involvement of the substrate-binding pocket in the binding event. Stronger competition is observed on addition of unlabelled αSyn, suggesting the existence of synergistic interactions stabilizing the αSyn/Hsp70 adduct. (**E**, **F**) Relative donor FRET respect to the Wt protein between Hsp70 and the N-terminally tagged αSyn (E, αSyn-24-AEDANS) or C-terminally tagged αSyn (F, αSyn-103-AEDANS) mutants lacking the hydrophobic region—residues 71–82—(ΔNAC mutants), in the absence or presence of ADP.

a shift in the binding equilibrium in the absence of one of these sites.

We note that the second identified segment (residues 71–82) spans a region that is absent in βSyn, a natural homologue of αSyn but which does not detectably aggregate under physiological conditions (Supplementary Figure 6A). FRET experiments carried out with three IAEDANS-labelled single-cysteine variants of βSyn, moreover, provided

evidence for the formation of a complex between βSyn and Hsp70 and showed the nucleotide dependence of the interaction involved (Supplementary Figure 6B). When compared with the equivalent experiment with αSyn, a similar FRET profile was observed for both complexes (see Figure 3B), except that the C-terminally labelled derivative (102 in αSyn and 103 in βSyn) showed significantly lower FRET efficiency for βSyn than for αSyn. This difference is more pronounced in the absence of nucleotides and likely reflects the sequence variations at the C-termini of both proteins as well as it strongly supports the involvement of the C-terminus of αSyn in the interaction with nucleotide-free Hsp70. Taken together, these results indicate that ADP-Hsp70 interacts with both predicted regions of αSyn, whereas nucleotide-free Hsp70 could interact, in addition, with the C-terminal tail of the protein.

Modulation of the anti-amyloid activity of Hsp70 by co-chaperones

The co-chaperone Hsp40 is generally thought to act together with Hsp70 and regulate complex formation with client polypeptides (Minami *et al*, 1996; Bukau and Horwich, 1998). To explore its effect on the anti-amyloidogenic capabilities of Hsp70, we performed experiments in which Hsp40 was included in solutions of aggregating αSyn and Hsp70. The addition of Hsp40, however, had no detectable effect on the conversion of αSyn into fibrils, and did not modify the chaperone activity of Hsp70, either in the free or in the nucleotide-bound states (Supplementary Figure 6C).

Recently, the Hsp70-interacting protein Hip (ST13) has been found to be significantly under-expressed in serum taken from patients suffering from PD (Scherzer *et al*, 2007). Hip modulates Hsp70 chaperone activity both *in vitro* (Hohfeld *et al*, 1995) and *in vivo* (Nollen *et al*, 2001), by interacting with the ATPase domain of the chaperone in its ADP-bound state (Hohfeld *et al*, 1995). As nothing is yet known concerning the possible effects of Hip on the anti-amyloidogenic activity of Hsp70, we have investigated this interaction further. Remarkably, we observed that the addition of Hip to Hsp70 in the presence of ATP results in the complete suppression of the conversion of αSyn into amyloid species as assayed by ThT fluorescence (Figure 4A). TEM analysis further shows that the presence of Hip and nucleotide-loaded Hsp70 resulted in the formation of small amorphous aggregates without fibrils (Figure 4B). The anti-amyloidogenic activity of Hip is mediated by Hsp70, because treatment with Hip alone did not inhibit the formation of αSyn fibrils. Moreover, Hip-mediated stabilization of Hsp70

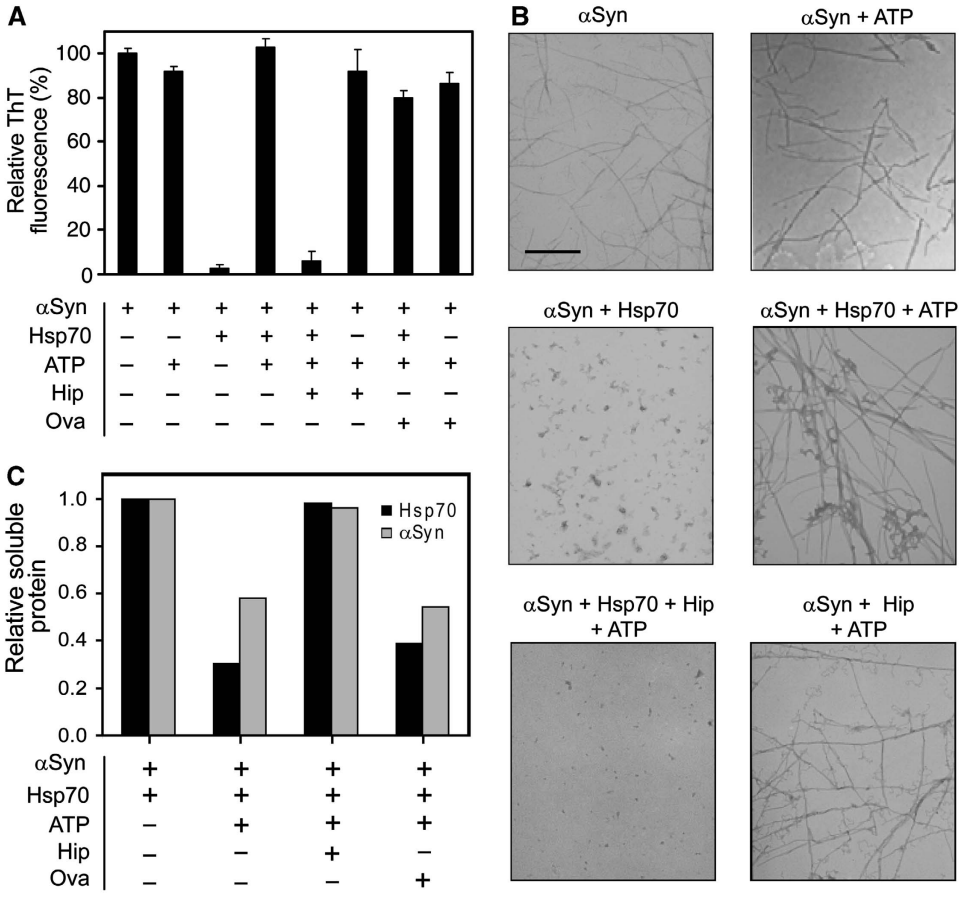

Figure 4 Suppression of the amyloid-dependent depletion of Hsp70 by Hip. (**A**) Bar diagram representing the relative ThT fluorescence levels reached at the end of the αSyn aggregation reaction. ATP was added to the mixture as indicated. In some samples, Hsp70 and/or Hip were included in the reaction mixture at a 1:10 molar ratio relative to αSyn. Error bars denote one s.d. from the mean calculated from two independent experiments. (**B**) TEM representative images of αSyn aggregates corresponding to the samples analysed in (A), at the end of the reaction. Scale bar: 500 nm. (**C**) Quantitative determination of soluble protein by densitometric analysis from a SDS–PAGE gel of the soluble fractions, at the end of the aggregation reaction represented in (A), relative to the initial concentration (see gel picture in Supplementary Figure 6D).

completely abrogated the chaperone co-aggregation that occurs in the presence of ATP, and appears to act by maintaining both αSyn and Hsp70 in solution (Figure 4C; Supplementary Figure 6D). This data suggests that Hip exerts a stabilizing effect on Hsp70 that supports chaperone-mediated inhibition of amyloid formation.

Inactivation of Hip increases α-Syn inclusion formation in C. elegans in an Hsp70-dependent manner

To establish the relevance of the anti-amyloidogenic function of the Hsp70/Hip complex *in vivo*, we have exploited a *C. elegans* model of αSyn inclusion formation (van Ham *et al*, 2008) and used knock-down techniques to suppress expression of orthologs of these genes (Figure 5). Depletion of Hsp70 (C12C8.1) caused a nonsignificant increase in the number of inclusions (1.4-fold) visible by confocal microscopy, suggesting redundancy in the anti-amyloidogenic function of chaperones. Conversely, knock-down of *hip* (T12D8.8) significantly increased the number of inclusions (2.3-fold; $P \leqslant 0.0001$), suggesting a central function of Hip in suppressing αSyn aggregation *in vivo* (Figure 5A and B). As Hip acts upstream of Hsp70 in our model, the increase in αSyn inclusions may well be dependent on the formation of an Hsp70/Hip complex. Indeed, the double knock-down Δ*hsp70/hip* reduced the number of inclusions by almost 60% ($P \leqslant 0.01$) compared with the single knock-down Δ*hip* (Figure 5A and B), reaching a level similar to the knock-down Δ*hsp70* (a 10% increase, $P > 0.05$). The results have showed strong genetic evidence of interactions between Hip and Hsp70 such that the effects observed due to the absence of Hip largely depend on the presence of Hsp70 (Figure 5C).

Discussion

Although considerable efforts have been made to try to understand how Hsp70 prevents the misfolding and aggregation of proteins in the cell (Mayer and Bukau, 2005), much less emphasis has been placed on the mechanism underlying its modulatory activity in the context of amyloid formation and disease. In the case of an ATP-dependent chaperone, it is of particular significance to unravel regulatory effects associated with conformationally dynamic states. Here, we describe biochemical and biophysical experiments that demonstrate that the ability of Hsp70 to inhibit the aggregation of αSyn depends on factors such as nucleotide binding and the presence of the Hip co-chaperone, for which we provide additional evidence from an *in vivo* model of αSyn aggregation. These factors appear to modulate the outcome of the protein misfolding and aggregation process, hence precluding the formation of toxic oligomeric species, rather than inhibiting the elongation of mature amyloid fibrils that are likely to be much less harmful.

Earlier studies have shown that Hsp70 could inhibit the formation of αSyn amyloid fibrils in the absence of ATP by interacting with oligomeric αSyn and stimulating the formation of amorphous aggregates (Dedmon *et al*, 2005; Huang *et al*, 2006). The results we present here show that in the presence of physiological concentrations of ATP, Hsp70 significantly increases the lag phase associated with αSyn

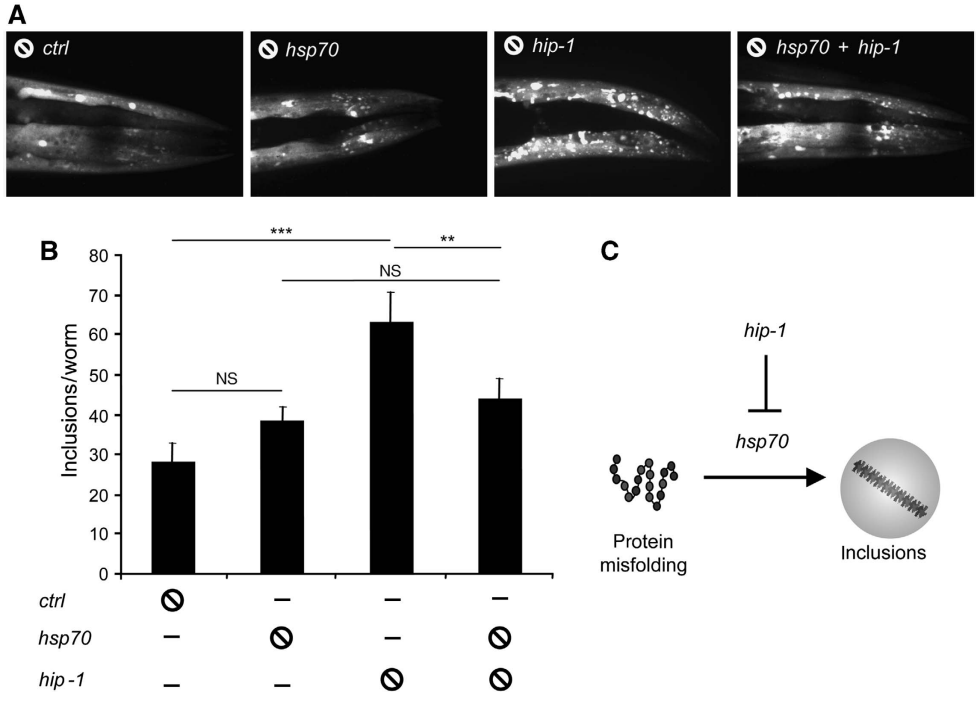

Figure 5 Increased αSyn inclusion formation in *C. elegans* follows inactivation of Hip in an Hsp70-dependent manner. (**A**) Confocal images showing the head regions of αSyn-YFP transgenic animals fed on bacteria expressing L4440 (empty vector) or RNAi targeting *hsp70* (C12C8.1), *hip* (T12D8.8) or a combination of *hsp70* and *hip*. Inclusion formation was quantified in age-synchronized young adult animals after growing on RNAi bacteria for two generations. (**B**) Quantification of the number of inclusions between the tip of the nose and the second pharyngeal bulb. Values indicated are mean numbers of inclusions, error bars represent the standard errors of the mean values (s.e.m.) [$n = 15$ (L4440), $n = 14$ (*hsp-70*), $n = 19$ (*hip-1*), $n = 16$ (*hsp-70 + hip-1*)]. $^{***}P \leqslant 0.0001$, $^{**}P \leqslant 0.01$ (Student's *t*-test). (**C**) Genetic model for the function of *hsp-70* and *hip-1* in inclusion formation representing the effect of Hip on the modulation of αSyn aggregation by Hsp70, in a PD scenario.

aggregation, such that amyloid fibrils still appear but typically much more slowly than when otherwise be the case (Figure 1). This finding is consistent with *in vivo* observations where over-expression of Hsp70 was found to reduce αSyn toxicity, but did not prevent the accumulation of amyloid aggregates in tissue (Auluck *et al*, 2002). We find the inhibitory effect of Hsp70 in the presence of ATP to be dependent on the Hsp70/αSyn ratio, and have observed that a combination of both αSyn and ATP, or its hydrolytic product ADP, causes Hsp70 itself to aggregate, regardless of the presence of Hsp40. These observations are in line with earlier findings related to HD, in which treatment of amyloidogenic huntingtin with Hsc70-Hsp40 and ATP disfavoured the population of oligomeric species and resulted in the accumulation of amyloid fibrils (Muchowski *et al*, 2000; Wacker *et al*, 2004). Moreover, the finding that Hsp70 has a tendency to aggregate in the presence of αSyn and ATP (or ADP) provides the basis for the well-established co-localization of Hsp70 and αSyn in Lewy bodies (Lee and Lee, 2002; Muchowski and Wacker, 2005). The depletion of functional chaperones and co-chaperones would heavily impair the ability of proteins to resist aggregation and to maintain protein homeostasis, phenomena that are thought to lie at the foundations of amyloid diseases (Dobson, 2003; Balch *et al*, 2008).

An interesting mechanistic observation from the current studies is that the addition of the competing peptide substrate NR does not detectably disrupt the efficacy of Hsp70 to act as a chaperone towards αSyn in the nucleotide-free state, and still allows the inhibition of amyloid formation by Hsp70. In the nucleotide-loaded state, however, the NR peptide reduces the extent of the co-aggregation of Hsp70 with αSyn (Figure 1), probably by competing with the protein for the substrate-binding pocket (Figure 3). These results suggest strongly the existence of distinct modes of binding for αSyn to nucleotide-loaded or nucleotide-free Hsp70, i.e. canonical and non-canonical binding modes, which are likely to determine the result of the aggregation reaction (Figure 6). FRET and NMR spectroscopy have enabled us to discover that Hsp70 does indeed recognize and bind to αSyn monomers as well as oligomers through at least three different types of interactions (Figure 3; Supplementary Figures 3–5). In the ADP-loaded state, αSyn monomers are located closer to the substrate-binding pocket of Hsp70, an interaction mediated by two regions, present in the N-terminal and NAC region of αSyn. We propose that this compact nucleotide-Hsp70/monomeric αSyn complex is critical in delaying the onset of fibril formation, but could also be responsible for the co-aggregation of Hsp70 and αSyn. A recent study mapped the region recognized on αSyn by Hsp70 as the broad segment between residues 21 and 110 (Luk *et al*, 2008). We have refined this region and located two stretches of amino acids with the highest probability of binding (residues 32–43 and 71–83) and then show that Hsp70 binds to the latter site, the stretch of hydrophobic residues that readily forms amyloid fibrils *in vitro*, and is generally assumed to be involved in initiating the conversion of αSyn into amyloid fibrils (Biere *et al*, 2000; Giasson *et al*, 2001). Moreover, binding to the N-terminal region of αSyn is supported by a comparative study of βSyn, in which we provide evidence of a complex formed with Hsp70, dispelling the general assumption that such an interaction is unlikely to occur.

Although likely to be less physiologically relevant, we have found that nucleotide-free Hsp70 also interacts with monomeric αSyn through which appears to be a non-canonical mode of interaction. This leads to the stabilization of soluble amorphous aggregates and hence inhibits fibril formation. These results are in line with the proposition (Gao *et al*, 1995) that when the nucleotide is absent from the nucleotide-binding site of Hsc70—the constitutively expressed analogue

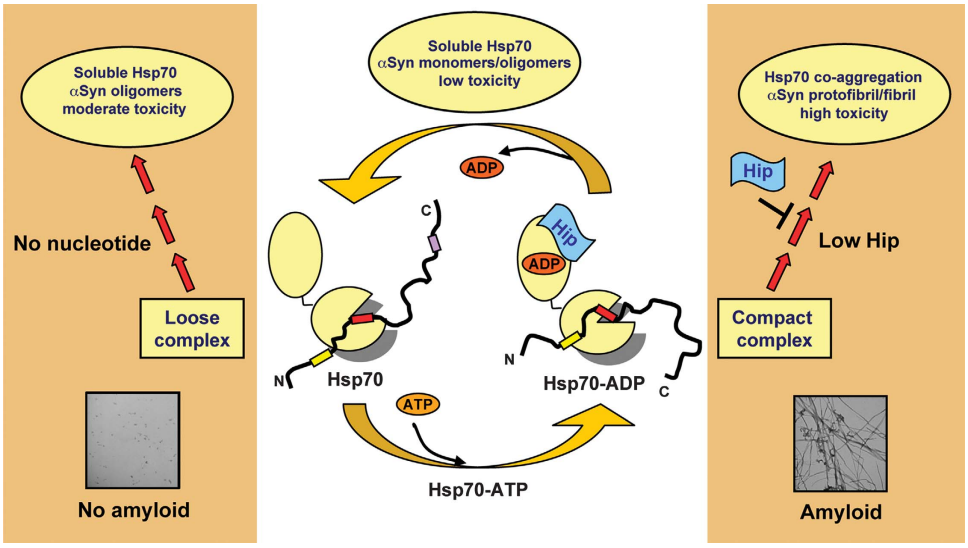

Figure 6 Proposed model for Hsp70-mediated modulation of αSyn aggregation. As Hsp70 cycles through the different nucleotide states sampling different conformations, it is able to inhibit αSyn aggregation by maintaining αSyn in a soluble conformation with low cytotoxicity (centre of cartoon). Depending on the nucleotide environment, there are different scenarios: (I) nucleotide-free Hsp70/αSyn forms a loose complex, which does not affect the solubility of Hsp70, and gives rise to disordered, soluble αSyn oligomers of moderate toxicity (left); (II) the compact ADP-Hsp70/αSyn complex, on the other hand, may lead to the co-aggregation of Hsp70 with αSyn, depleting the chaperone from solution, and allowing αSyn fibrils to form rapidly, a process that populates intermediates with high cytotoxicity (right). The co-chaperone Hip, on binding to the ATPase domain of Hsp70 in the ADP-state, could stabilize the ADP-Hsp70 complex and maintain Hsp70 in solution, hence inhibiting the pathway towards αSyn fibril formation. The denomination of 'loose' and 'compact' complex originates from the determination of a set of FRET-derived intermolecular distances for the Hsp70/αSyn interaction in the absence and presence of ADP, respectively (see Supplementary data and Supplementary Figure 4C).

of Hsp70—the substrate-binding region interacts more flexibly with a protein substrate. Possibly such transient interactions, recently suggested for the Hsp70/αSyn complex (Luk *et al*, 2008), do not compromise the solubility of Hsp70. With ADP in the nucleotide-binding site, however, the SBD appears to be much less dynamic, as the residence time of the substrate in the binding pocket is increased. Finally, the FRET data suggest that αSyn oligomers are preferentially bound by nucleotide-free Hsp70, consistent with the view that N-terminal and central domains of αSyn are likely to be buried in the aggregated species.

One possible reason why nucleotide-free Hsp70 impairs the ability of αSyn to form amyloid fibrils could be related to an off-pathway nature of the intermediate species stabilized by the formation of the Hsp70/αSyn complex. Indeed, we observed non-fibrillar oligomers to be predominantly populated at early incubation time points in the presence of nucleotide-free chaperone, whereas short protofibrils of αSyn were found to co-aggregate with Hsp70 in the presence of ATP. Studies of the effects of such soluble pre-fibrillar aggregates on a human neuronal cell line have shown that protofibrils initially formed by treatment with Hsp70 and ATP are less toxic than the oligomers stabilized by nucleotide-free Hsp70 (Figure 2). This protective effect of Hsp70 in a medium with ATP, however, disappears during the course of the elongation phase of fibril formation in parallel with the depletion of soluble Hsp70. A shift in population towards highly toxic soluble αSyn species at later points in the aggregation reaction suggests that Hsp70 is co-aggregating with less toxic αSyn species.

Biologically, Hsp70 does not function independently as many co-chaperones and auxiliary factors are involved in regulating its cellular functions in the cell. In this regard, it is extremely interesting that the Hsp70-interacting protein Hip (ST13) has recently been found to be consistently under-expressed in PD patients even in the early stages of the disease (Scherzer *et al*, 2007), a conclusion that suggests a coupling between both proteins in disease progression or initiation. We have found strong evidence in this study for a dramatic effect of Hip on the availability of functionally competent Hsp70 in the presence of aggregating αSyn. Hip is in fact capable of suppressing the co-aggregation of Hsp70 with αSyn, and hence the extent of amyloid fibril formation observed in the presence of nucleotides is virtually completely suppressed in the presence of Hip (Figure 4). Moreover, our results with an *in vivo* αSyn aggregation model of *C. elegans* strongly support the hypothesis derived from the *in vitro* experiments, indicating that Hip is indeed required for suppression of αSyn inclusion formation in an Hsp70-dependent manner (Figure 5). In line with this important finding, a recent study of a polyQ model of HD found that Hip assists Hsp70 in the anti-aggregation activity of Hsp70 (Howarth *et al*, 2009). The observation in our *C. elegans* model that the absence of Hip alone could give rise to more inclusions than when both Hip and Hsp70 are absent is consistent with a scenario in which there is a redundancy of chaperone pathways, likely mediated by the constitutive presence of Hsc70 and other chaperones such as Hsp90 (Uryu *et al*, 2006). Interestingly, Hip has been shown to interact with Hsp70 by binding to its ATPase domain specifically in the ADP-bound state, both *in vitro* and *in vivo*, without affecting its ATPase activity (Hohfeld *et al*, 1995; Nollen *et al*, 2001). A possible explanation for its stabilizing effect on the ADP-Hsp70/αSyn complex in solution is that the binding of Hip could shield hydrophobic regions in the ATPase domain of Hsp70 that become exposed in the ADP-bound complex with αSyn (Figure 6). Alternatively, we speculate that binding of Hip to the ATPase domain could induce a structural change in the SBD, favouring a conformation of Hsp70 similar to that populated in the nucleotide-free state, which we have shown does not promote the co-aggregation of Hsp70 and αSyn. This situation could be reminiscent of that proposed for the Hsp70 escorting protein (Hep) when bound to the nucleotide-free state of mitochondrial Hsp70 (mtHsp70), which inhibits self-aggregation of mtHsp70, both *in vitro* and *in vivo* (Sichting *et al*, 2005).

In summary, three central conclusions from this study appear to be of broad importance in the quest to unravel the highly complex function of chaperone availability and proteostasis in amyloid diseases. The first is the observation that the ATP cycle modulates the ability of Hsp70 to inhibit fibril formation by amyloid-forming proteins, shedding light on the mechanism by which ATP-dependent chaperones act in the context of misfolding diseases. The second important finding is that ADP-bound Hsp70 has a very high propensity to co-aggregate with αSyn, suggesting that chaperone depletion favoured under certain conditions could be an important feature in the onset and progression of amyloid disorders. Finally, we have identified a functional role of Hip, an auxiliary factor for Hsp70, in preventing the co-aggregation of Hsp70 with αSyn, thereby reducing the toxicity of amyloidogenesis. Maintaining the cellular level of Hip may be one solution for intervening the onset and development of PD.

Materials and methods

Further details of the Materials and methods are provided in Supplementary data.

Materials

ATP, ADP and ThT were purchased from Sigma. Adenosine-5′-O-(3-thio triphosphate) (ATPγS, >90% purity, HPLC-purified) was purchased from Roche. The NR peptide (H_2N-NRLLLTG-COOH) was synthesized and purified (>95% purity) by Genemed Synthesis Inc. (USA). IAEDANS and 5-(dimethylamino)naphthalene-1-sulfonylmethyl sulfoxide (DANSYL-MTS) were obtained from Invitrogen and Toronto Research, respectively.

Protein expression and purification

Human cytoplasmic Hsp70 (Hsp70 1A, gi:194248072) was expressed, purified and characterized as described in Supplementary data. Recombinant human Hsp40 and purified rat Hip were obtained from Stressgen (#SPP-400 and SPP-767, respectively). The wild-type human αSyn (gi:80475099) or βSyn (gi:12804099) genes were inserted in pT7-7 and pRK172 vectors, respectively, and subsequently expressed and purified as described earlier (Rivers *et al*, 2008). Protein purity exceeded 95% as determined by SDS–PAGE, and the αSyn concentration was determined from the absorbance measurements at 275 nm using an extinction coefficient of 5400 $M^{-1}cm^{-1}$.

αSyn aggregation experiments

Solutions for aggregation experiments contained 70 μM αSyn alone or together with 7 μM Hsp70 (except where a ratio other than 1:10 is indicated) in 50 mM Tris (pH 7.4), 50 mM KCl, 2 mM $MgCl_2$, 0.35 mM SDS and 0.02% NaN_3. Where indicated, samples contained and ATP-regeneration system: 0.2 units/ml pyruvate kinase and 5 mM phosphoenol pyruvate, in the absence or presence of 2 mM ATP (or ADP or ATPγS). Alternatively, reactions were carried out in the presence of 5 mM nucleotide in the absence of an ATP-regeneration system. Formation of fibrils by α-Syn was monitored by measuring ThT fluorescence and fitting to the kinetics followed a nucleation polimerization model as described elsewhere (Rivers *et al*, 2008). For kinetic aggregation studies using SDS, either two or three replicas were used for each set of conditions. In these samples, 20 μM ThT was included before initiating the

aggregation reaction. Aggregation was induced by heating the samples in a 96-well plate to 37°C while shaking, and readings were taken every ~7 min in a FluoStar OPTIMA spectrophotometer with excitation and emission windows at 440 ± 10 and 480 ± 10 nm, respectively, and an averaging time of 20 s. For kinetic studies in the absence of SDS, aggregation was induced by magnetic stirring at 37°C, and ThT was measured in a Cary Eclipse spectrofluorimeter with an excitation wavelength of 440 nm (slit-width 5 nm) and an emission scan from 450 to 600 nm (slit-width 5 nm). It might be relevant to note that this Hsp70-ATP-dependent, αSyn fibril formation was not related to the presence or absence of SDS in the reaction mixture (Supplementary Figure 2A).

SDS–PAGE analysis

Samples were analysed by SDS–PAGE using 4–12% Bis-Tris NuPAGE gels (Invitrogen) in MES buffer under reducing conditions. Gels were stained using Coomassie brilliant blue dye. Densitometry analysis was performed on scanned gels (Supplementary Figures 2 and 6) using the Image J (NIH) software.

Cytotoxicity assays

Samples for cytotoxicity assays were taken from aggregation assays performed in the absence of ThT. Aliquots were removed at 0, 4, 8, 24, 42 and 64 h time periods and subjected to electron microscopy, *ex situ* measurement of ThT fluorescence intensity, and the remaining stored at −80°C for cytotoxicity studies. Where required, samples were centrifuged at 16 000 × *g* for 10 min to separate the aggregates into insoluble and soluble fractions. The retention of aggregate morphology after freeze/thawing was confirmed by electron microscopy (not shown). LDH was measured on SH-SY5Y cells as a way of parametrizing the differential toxicity of aggregated samples on the viability, as described in Supplementary data.

Protein labelling and purification of oligomers

Labelling of αSyn and βSyn cysteine mutants with IAEDANS or DANSYL-MTS was performed as follows: 1–5 mg of lyophilized Cys-containing proteins were dissolved in PBS and 5 mM DTT was added to ensure complete reduction of the sole cysteine residue. DTT was removed by gel filtration in PD10 columns (GE Healthcare) and a five-fold molar excess of the dye (dissolved in DMSO) was then added immediately. Conjugation of the dye was optimized by overnight incubation at 4°C in the dark. Excess dye was removed by performing an added gel filtration step using PD10 columns (Sepharose G-25). The eluted proteins were subjected to size exclusion in an analytical Superdex 75 column (GE Healthcare) to separate oligomeric and monomeric species. Proteins were concentrated by centrifugal devices (10 kDa cut-off for monomer and 100 kDa for oligomers) and stored at −80°C. Labelling efficiency was typically found to be between 60 and 95%.

Fluorescence spectroscopy

For FRET experiments, the tryptophan residues of Hsp70 acted as donors and AEDANS as acceptors (Jeganathan *et al*, 2006), using AEDANS-labelled αSyn or βSyn cysteine-mutants. In all the experiments, FRET was determined as donor desensitization, except for the case of the aggregation experiments, where amyloid-dependent insolubility of Hsp70 precluded the accurate determination of donor quenching. In this case, the acceptor sensitization method was used. For determinations of the relative affinity of the αSyn/Hsp70 complex, αSyn cysteine mutants labelled with the DANSYL fluorophore were used.

Transmission electron microscopy

Samples were prepared from 10 μl aliquots of aggregation reactions using negative staining by 2% (w/v) uranyl acetate on Formvar/carbon-coated copper grids (Agar Scientific). Images were obtained at × 25 000 magnification using a Phillips CEM100 transmission electron microscope.

C. elegans strain and RNAi

The transgenic αSyn strain used for RNAi experiments, OW40 (OW40 zgIs15[P(unc-54)::α-synuclein::YFP(xScaI)N2(xPvuII)] was created by microinjection and integrated by γ-irradiation. Synchronized larvae were fed on bacterial strains expressing double-stranded RNA as described earlier (van Ham *et al*, 2008). An RNAi clone targeting *hsp-70* (C12C8.1) was obtained from the Ahringer bacterial RNAi library. We constructed an RNAi clone targeting *hip-1* (T12D8.8) by cloning an ~1000 bp DNA fragment (generated by PCR amplification with primers: T12D8.8_F: 5′-CTAAGCTAGCGAA AATGGACCACGTCGC ATTG-3′ and T12D8.8_R: 5′-GATACTCGAGAC TTGTCTTGTCGCGAAGCA-3′ into L4440. Worms were grown on the different RNAi clones and allowed to have progeny. L4 progeny (second generation) was transferred to new RNAi agar plates and inclusions were quantified in age-synchronized adults. All gene targets of the positive-RNAi used for feeding were verified by sequencing of the insert of the RNAi plasmids.

Solamere confocal laser scanning microscopy

Transgenic animals were mounted on glass microscope slides on 2% agarose pads containing 40 mM NaN_3 as an anaesthetic. Animals were imaged using a Solamere Nipkow confocal live cell imaging system (Solamere, USA) based on a Leica DM IRE2 inverted confocal microscope with a 40× oil immersion objective (HCX PL APO CS). Images shown are 2D maximal projections of z-stacks and were captured using *In Vivo*3 Software (Mediacybernetics, USA). For quantification of the number of inclusions, all distinct foci between the nose and second pharyngeal bulb were counted. Measurements on inclusions were performed using ImageJ software. Statistical significance was determined using Student's *t*-tests.

Supplementary data

Supplementary data are available at *The EMBO Journal* Online (http://www.embojournal.org).

Acknowledgements

We are grateful to Drs Robert Rivers, Xavier Salvatella and Sophie Jackson for reagents and discussions. We acknowledge with gratitude the use of the Biomolecular NMR Facility, Department of Chemistry, University of Cambridge, at Cambridge, UK, and the advice of the staff. We thank K Sjollema from the UMCG Microscopy and Imaging Center (UMIC) for advice on microscopy. CR and AA held FEBS Long-Term Fellowships. CWB is an EMBO Long-Term Postdoctoral Fellow, ATvdG was the recipient of a Topmaster fellowship of the graduate school GUIDE for Drug Exploration of the University of Groningen. STDH is a recipient of a Human Frontier Science Program Long-termFellowship (LT0798/2005) and is supported in part by the National Science Council of the Republic of China, Taiwan(NSC97-2917-1-564-102). JC is recipient of a Human Frontier Young Investigators Award (RGY67/2007) and also thanks the BBSRC (9015651/1). CMD and JC acknowledge funding from The Wellcome Trust and The Leverhulme Trust. DP is grateful to The Spanish Ministry of Health (PI05/2056; PI06/1641), The Spanish Ministry of Science and Innovation (SAF2007-29418E) and the PAIDI Program from the Regional Government (BIO323) for funding. EAAN acknowledges ZonMW Research Institute of Diseases in the Elderly and De Nederlandse Hersenstichting for funding.

Conflict of interest

The authors declare that they have no conflict of interest.

References

Auluck PK, Chan HY, Trojanowski JQ, Lee VM, Bonini NM (2002) Chaperone suppression of alpha-synuclein toxicity in a Drosophila model for Parkinson's disease. *Science* **295:** 865–868

Balch WE, Morimoto RI, Dillin A, Kelly JW (2008) Adapting proteostasis for disease intervention. *Science* **319:** 916–919

Biere AL, Wood SJ, Wypych J, Steavenson S, Jiang Y, Anafi D, Jacobsen FW, Jarosinski MA, Wu GM, Louis JC, Martin F, Narhi LO, Citron M (2000) Parkinson's disease-associated alpha-synuclein is more fibrillogenic than beta- and gamma-synuclein and cannot cross-seed its homologs. *J Biol Chem* **275:** 34574–34579

Bukau B, Horwich AL (1998) The Hsp70 and Hsp60 chaperone machines. *Cell* **92:** 351–366

Chiti F, Dobson CM (2006) Protein misfolding, functional amyloid, and human disease. *Annu Rev Biochem* **75:** 333–366

Danzer KM, Haasen D, Karow AR, Moussaud S, Habeck M, Giese A, Kretzschmar H, Hengerer B, Kostka M (2007) Different species of alpha-synuclein oligomers induce calcium influx and seeding. *J Neurosci* **27:** 9220–9232

Dedmon MM, Christodoulou J, Wilson MR, Dobson CM (2005) Heat shock protein 70 inhibits alpha-synuclein fibril formation via preferential binding to prefibrillar species. *J Biol Chem* **280:** 14733–14740

Demuro A, Mina E, Kayed R, Milton SC, Parker I, Glabe CG (2005) Calcium dysregulation and membrane disruption as a ubiquitous neurotoxic mechanism of soluble amyloid oligomers. *J Biol Chem* **280:** 17294–17300

Dobson CM (2003) Protein folding and misfolding. *Nature* **426:** 884–890

Frydman J, Nimmesgern E, Ohtsuka K, Hartl FU (1994) Folding of nascent polypeptide chains in a high molecular mass assembly with molecular chaperones. *Nature* **370:** 111–117

Gao B, Eisenberg E, Greene L (1995) Interaction of nucleotide-free Hsc70 with clathrin and peptide and effect of ATP analogues. *Biochemistry* **34:** 11882–11888

Giasson BI, Murray IV, Trojanowski JQ, Lee VM (2001) A hydrophobic stretch of 12 amino acid residues in the middle of alpha-synuclein is essential for filament assembly. *J Biol Chem* **276:** 2380–2386

Gragerov A, Nudler E, Komissarova N, Gaitanaris GA, Gottesman ME, Nikiforov V (1992) Cooperation of GroEL/GroES and DnaK/DnaJ heat shock proteins in preventing protein misfolding in Escherichia coli. *Proc Natl Acad Sci USA* **89:** 10341–10344

Gragerov A, Zeng L, Zhao X, Burkholder W, Gottesman ME (1994) Specificity of DnaK-peptide binding. *J Mol Biol* **235:** 848–854

Greene LE, Zinner R, Naficy S, Eisenberg E (1995) Effect of nucleotide on the binding of peptides to 70-kDa heat shock protein. *J Biol Chem* **270:** 2967–2973

Grunblatt E, Mandel S, Maor G, Youdim MB (2001) Gene expression analysis in N-methyl-4-phenyl-1,2,3,6-tetrahydropyridine mice model of Parkinson's disease using cDNA microarray: effect of R-apomorphine. *J Neurochem* **78:** 1–12

Hartl FU (1996) Molecular chaperones in cellular protein folding. *Nature* **381:** 571–579

Hauser MA, Li YJ, Xu H, Noureddine MA, Shao YS, Gullans SR, Scherzer CR, Jensen RV, McLaurin AC, Gibson JR, Scott BL, Jewett RM, Stenger JE, Schmechel DE, Hulette CM, Vance JM (2005) Expression profiling of substantia nigra in Parkinson disease, progressive supranuclear palsy, and frontotemporal dementia with parkinsonism. *Arch Neurol* **62:** 917–921

Hohfeld J, Minami Y, Hartl FU (1995) Hip, a novel cochaperone involved in the eukaryotic Hsc70/Hsp40 reaction cycle. *Cell* **83:** 589–598

Howarth JL, Glover CP, Uney JB (2009) HSP70 interacting protein prevents the accumulation of inclusions in polyglutamine disease. *J Neurochem* **108:** 945–951

Hsu ST, Bertoncini CW, Dobson CM (2009) Use of protonless NMR spectroscopy to alleviate the loss of information resulting from exchange-broadening. *J Am Chem Soc* **131:** 7222–7223

Huang C, Cheng H, Hao S, Zhou H, Zhang X, Gao J, Sun QH, Hu H, Wang CC (2006) Heat shock protein 70 inhibits alpha-synuclein fibril formation via interactions with diverse intermediates. *J Mol Biol* **364:** 323–336

Jeganathan S, von Bergen M, Brutlach H, Steinhoff HJ, Mandelkow E (2006) Global hairpin folding of tau in solution. *Biochemistry* **45:** 2283–2293

Klucken J, Outeiro TF, Nguyen P, McLean PJ, Hyman BT (2006) Detection of novel intracellular alpha-synuclein oligomeric species by fluorescence lifetime imaging. *FASEB J* **20:** 2050–2057

Klucken J, Shin Y, Masliah E, Hyman BT, McLean PJ (2004) Hsp70 reduces alpha-synuclein aggregation and toxicity. *J Biol Chem* **279:** 25497–25502

Lashuel HA, Lansbury Jr PT (2006) Are amyloid diseases caused by protein aggregates that mimic bacterial pore-forming toxins? *Q Rev Biophys* **39:** 167–201

Lashuel HA, Petre BM, Wall J, Simon M, Nowak RJ, Walz T, Lansbury Jr PT (2002) Alpha-synuclein, especially the Parkinson's disease-associated mutants, forms pore-like annular and tubular protofibrils. *J Mol Biol* **322:** 1089–1102

Lee HJ, Lee SJ (2002) Characterization of cytoplasmic alpha-synuclein aggregates. Fibril formation is tightly linked to the inclusion-forming process in cells. *J Biol Chem* **277:** 48976–48983

Luheshi LM, Crowther DC, Dobson CM (2008) Protein misfolding and disease: from the test tube to the organism. *Curr Opin Chem Biol* **12:** 25–31

Luk KC, Mills IP, Trojanowski JQ, Lee VM (2008) Interactions between Hsp70 and the hydrophobic core of alpha-synuclein inhibit fibril assembly. *Biochemistry* **47:** 12614–12625

Macario AJ, De Macario EC (2007) Chaperonopathies by defect, excess, or mistake. *Ann N Y Acad Sci* **1113:** 178–191

Maeda H, Sahara H, Mori Y, Torigo T, Kamiguchi K, Tamura Y, Tamura Y, Hirata K, Sato N (2007) Biological heterogeneity of the peptide-binding motif of the 70-kDa heat shock protein by surface plasmon resonance analysis. *J Biol Chem* **282:** 26956–26962

Matsumoto S, Hammes GG (1975) Fluorescence energy transfer between ligand binding sites on aspartate transcarbamylase. *Biochemistry* **14:** 214–224

Mayer MP, Brehmer D, Gassler CS, Bukau B (2001) Hsp70 chaperone machines. *Adv Protein Chem* **59:** 1–44

Mayer MP, Bukau B (2005) Hsp70 chaperones: cellular functions and molecular mechanism. *Cell Mol Life Sci* **62:** 670–684

Minami Y, Hohfeld J, Ohtsuka K, Hartl FU (1996) Regulation of the heat-shock protein 70 reaction cycle by the mammalian DnaJ homolog, Hsp40. *J Biol Chem* **271:** 19617–19624

Mogk A, Tomoyasu T, Goloubinoff P, Rudiger S, Roder D, Langen H, Bukau B (1999) Identification of thermolabile Escherichia coli proteins: prevention and reversion of aggregation by DnaK and ClpB. *EMBO J* **18:** 6934–6949

Muchowski PJ, Schaffar G, Sittler A, Wanker EE, Hayer-Hartl MK, Hartl FU (2000) Hsp70 and hsp40 chaperones can inhibit self-assembly of polyglutamine proteins into amyloid-like fibrils. *Proc Natl Acad Sci USA* **97:** 7841–7846

Muchowski PJ, Wacker JL (2005) Modulation of neurodegeneration by molecular chaperones. *Nat Rev Neurosci* **6:** 11–22

Nollen EA, Kabakov AE, Brunsting JF, Kanon B, Hohfeld J, Kampinga HH (2001) Modulation of *in vivo* HSP70 chaperone activity by Hip and Bag-1. *J Biol Chem* **276:** 4677–4682

Palleros DR, Reid KL, Shi L, Welch WJ, Fink AL (1993) ATP-induced protein-Hsp70 complex dissociation requires K+ but not ATP hydrolysis. *Nature* **365:** 664–666

Rivers RC, Kumita JR, Tartaglia GG, Dedmon MM, Pawar A, Vendruscolo M, Dobson CM, Christodoulou J (2008) Molecular determinants of the aggregation behavior of alpha- and beta-synuclein. *Protein Sci* **17:** 887–898

Rudiger S, Buchberger A, Bukau B (1997a) Interaction of Hsp70 chaperones with substrates. *Nat Struct Biol* **4:** 342–349

Rudiger S, Germeroth L, Schneider-Mergener J, Bukau B (1997b) Substrate specificity of the DnaK chaperone determined by screening cellulose-bound peptide libraries. *EMBO J* **16:** 1501–1507

Saibil HR (2008) Chaperone machines in action. *Curr Opin Struct Biol* **18:** 35–42

Scherzer CR, Eklund AC, Morse LJ, Liao Z, Locascio JJ, Fefer D, Schwarzschild MA, Schlossmacher MG, Hauser MA, Vance JM, Sudarsky LR, Standaert DG, Growdon JH, Jensen RV, Gullans SR (2007) Molecular markers of early Parkinson's disease based on gene expression in blood. *Proc Natl Acad Sci USA* **104:** 955–960

Scheufler C, Brinker A, Bourenkov G, Pegoraro S, Moroder L, Bartunik H, Hartl FU, Moarefi I (2000) Structure of TPR domain-peptide complexes: critical elements in the assembly of the Hsp70-Hsp90 multichaperone machine. *Cell* **101:** 199–210

Sichting M, Mokranjac D, Azem A, Neupert W, Hell K (2005) Maintenance of structure and function of mitochondrial Hsp70 chaperones requires the chaperone Hep1. *EMBO J* **24:** 1046–1056

Stefani M, Dobson CM (2003) Protein aggregation and aggregate toxicity: new insights into protein folding, misfolding diseases and biological evolution. *J Mol Med* **81:** 678–699

Takayama S, Reed JC (2001) Molecular chaperone targeting and regulation by BAG family proteins. *Nat Cell Biol* **3:** E237–E241

Uryu K, Richter-Landsberg C, Welch W, Sun E, Goldbaum O, Norris EH, Pham CT, Yazawa I, Hilburger K, Micsenyi M, Giasson BI, Bonini NM, Lee VM, Trojanowski JQ (2006) Convergence of

heat shock protein 90 with ubiquitin in filamentous alpha-synuclein inclusions of alpha-synucleinopathies. *Am J Pathol* **168:** 947–961

van Ham TJ, Thijssen KL, Breitling R, Hofstra RM, Plasterk RH, Nollen EA (2008) C. elegans model identifies genetic modifiers of alpha-synuclein inclusion formation during aging. *PLoS Genet* **4:** e1000027

Wacker JL, Zareie MH, Fong H, Sarikaya M, Muchowski PJ (2004) Hsp70 and Hsp40 attenuate formation of spherical and annular polyglutamine oligomers by partitioning monomer. *Nat Struct Mol Biol* **11:** 1215–1222

Young JC, Agashe VR, Siegers K, Hartl FU (2004) Pathways of chaperone-mediated protein folding in the cytosol. *Nat Rev Mol Cell Biol* **5:** 781–791

Zhou Y, Gu G, Goodlett DR, Zhang T, Pan C, Montine TJ, Montine KS, Aebersold RH, Zhang J (2004) Analysis of alpha-synuclein-associated proteins by quantitative proteomics. *J Biol Chem* **279:** 39155–39164

